Reanalysis of muonic ^{90}Zr and ^{208}Pb atoms

Akihiro Haga,[1,*] Yataro Horikawa,[2,†] and Hiroshi Toki[1,‡]
[1]*Research Center for Nuclear Physics (RCNP), Osaka University, Ibaraki, Osaka 567-0047, Japan*
[2]*Department of Physics, Juntendo University, Inba-gun, Chiba 270-1695, Japan*
(Received 10 December 2006; published 26 April 2007)

Muonic transition energies in lowlying $\mu^- - ^{90}$Zr and $\mu^- - ^{208}$Pb states are reanalyzed by using nuclear polarization with the full-electromagnetic nuclear response. The possibility of the observed enhancement of the energy-weighted sum rule is also considered in the analysis. The transverse part of the nuclear polarization and the enhancement effect play an important role in improving the fine structure splitting of muonic p-states in both nuclei. Furthermore, introducing a pygmy dipole resonance in the excitation spectrum, the final fit drastically improves in ^{208}Pb. However, there remains a discrepancy in ^{90}Zr, for which the structure of the nuclear excitation spectrum is insensitive to the nuclear-polarization energy shift. Therefore, the remaining discrepancy might be caused by effects other than the nuclear polarization.

DOI: 10.1103/PhysRevC.75.044315 PACS number(s): 31.30.Jv, 32.10.Fn, 12.20.Ds

I. INTRODUCTION

The energy level of muonic atoms contains various information regarding quantum electrodynamics (QED), atomic and nuclear physics. The uncertainty of muonic levels in heavy nuclei is mainly ascribed to the nuclear structure, and thus it has been considered that muonic atoms could be one of the tools for investigating the electromagnetic properties of nuclei. For instance, the muonic atom has been shown to contribute to the determination of nuclear charge radii [1]. As the precision of measurement has increased, however, it has been found that there is a discrepancy between experimental results and theoretical results of the nuclear polarization (NP) correction. The discrepancy of the NP correction for the muonic x-ray analysis was first reported in the $\Delta 2p$ splitting energy of ^{208}Pb [2]. In that analysis, the charge distribution determined from elastic electron scattering and muonic x-ray data was used and muonic transition energies with all corrections other than the NP correction were evaluated, and then the experimentally allowable values of the NP corrections were deduced. The analysis gave the opposite result from the theoretical NP prediction of those days: while the calculation predicted a larger NP energy for $2p_{1/2}$ than for $2p_{3/2}$, the experimental analysis gave a smaller NP energy for $2p_{1/2}$ than for $2p_{3/2}$ [3]. The same kind of discrepancies were pointed out in the muonic $2p$ level of ^{90}Zr [4]. Furthermore, a serious problem has been found in the new x-ray measurement for muonic ^{208}Pb; that is, there is a discrepancy also in the $\Delta 3p$ splitting energy. It amounts to 300–500 eV, which is almost the same magnitude as that of the $\Delta 2p$ splitting energy [5].

The analyses of the NP correction described above were performed with the longitudinal nuclear response function only, which never provides a muon-spin dependence, under the assumption that the nuclear-muon dynamics would be nonrelativistic. An attempt to cure discrepancies of muonic levels with the transverse part of the nuclear response has been done recently in ^{208}Pb by respecting the gauge invariance of the NP correction [6]. The transverse NP correction drastically reduces the binding energy for the $p_{1/2}$ state, and as a result, it has improved about half of the anomaly in the $\Delta 2p$ splitting. However, the discrepancy has still remained. In addition, the calculation has shown that the $\Delta 3p$ splitting was not improved because the absolute value of the NP correction in $3p$ states is three-times smaller than that in $2p$ states [3,6,7]. Thus, these discrepancies remain long-standing unsolved anomalies in the observed heavy muonic data: the experimental analysis requires NP energy shifts for the fine structure opposite to those of the theoretical prediction, and the $3p$ splitting energy of ^{208}Pb due to NP correction should be of the same order of magnitude as the $2p$ splitting energy.

In this paper, we report on the reanalysis of the muonic energy levels in ^{90}Zr and ^{208}Pb, including two other effects in addition to the transverse effect for the NP correction; one is the effect of the enhanced energy-weighted sum rule (EWSR) and the other is the resonance effect with newly found nuclear states; pygmy dipole resonances (PDR) [8–10]. The former increases the overall energy shift due to the NP correction. Consequently, this makes the effect of the transverse NP correction large. The latter, the NP correction due to the PDR, is a promising candidate to resolve the anomaly that the $2p$ and $3p$ NP corrections in ^{208}Pb have almost the same magnitude, since the muonic $3p$ levels with excitation energy of about 8.5 MeV are able to resonate with this nuclear mode. On the other hand, the PDR cannot resonate with the muonic levels of lighter nuclei, hence it should have a minor role in Zr. Thus, it is interesting to investigate this effect in both Zr and Pb simultaneously.

In the present analysis, we employ collective models in the calculation of NP effects. There are some advantages in using collective models: It is crucial for the quantitative description in the energy shift of muonic levels to use the information obtained from the observed data such as the experimental excitation energy of, and transition strengths to the lowlying nuclear states. We can incorporate these effects in collective models without much computational effort, compared with the

*Electronic address: haga@rcnp.osaka-u.ac.jp
†Electronic address: horikawa@sakura.juntendo.ac.jp
‡Electronic address: toki@rcnp.osaka-u.ac.jp

microscopic calculations such as random-phase approximation (RPA). The disadvantage is that the transverse NP correction may be gauge-dependent, since we do not know how to construct gauge-invariant collective models. As has been verified in hydrogenlike atoms, however, the degree of this violation would be negligibly small with a suitable form of the transition density [11]. In the present paper, we will employ the three forms for the transition density and will confirm, by calculating both in the Feynman and Coulomb gauges, that the gauge dependence is negligible in the analysis of the muonic transition energies. These matters are discussed in some detail in Sec. II.

The muonic levels are affected by the QED and recoil corrections, and we have explained our treatment of these corrections in Sec. III. This would also be useful for conducting future work in this direction, since it is not clear to us at present whether or not improvement in the QED corrections may solve a part of the anomalies. In Sec. IV, we perform χ^2 fit to the experimental data for the muonic transition energies of Refs. [4] and [5] with respect to the parameters of the Fermi-type charge distribution of the nucleus, and discuss the anomalies in the Δp splittings. Finally, we give a summary of our analysis in Sec. V.

II. NUCLEAR POLARIZATION WITH COLLECTIVE MODELS

The diagrams of the leading-order NP corrections are depicted in Fig. 1, where the nuclear vertex has no diagonal matrix elements for the ladder [Fig. 1(a)], the cross [Fig. 1(b)], and the nuclear polarization combined vacuum polarization (NP-VP, Fig. 1(d) [12]) diagrams, and no nuclear intermediate state for the seagull [Fig. 1(c)] diagram. The seagull diagram, which does not polarize a nucleus, should be regarded as a part of the "nuclear polarization" correction because it plays a crucial role in retaining the gauge invariance of the NP correction [6,11,13–15]. While each correction due to Figs. 1(a)–1(c) is gauge-dependent, the sum of their corrections is gauge-invariant. The NP-VP correction is gauge-invariant itself. The effect of the NP-VP diagram to the muonic levels is different from that of the others, that is, the interaction with the muon is represented by the local potential. Therefore, it is expected that its contribution can be taken into account by renormalization of the parameters of the nuclear charge distribution. However, we will also treat the NP-VP diagram explicitly in order to make the analysis complete within a second-order perturbation by nuclear polarization.

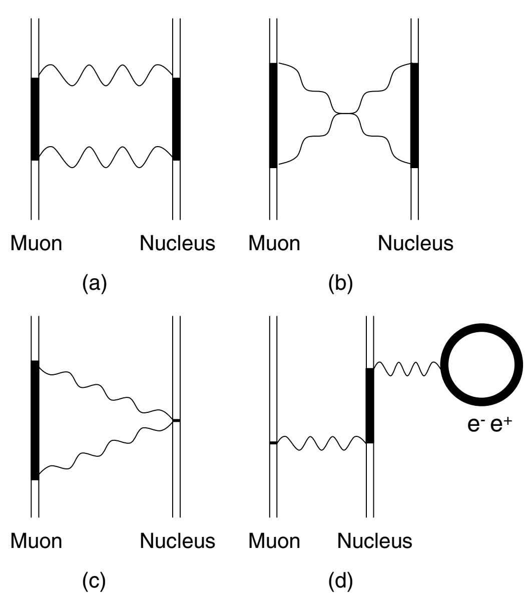

FIG. 1. Lowest-order nuclear polarization diagrams: (a) ladder, (b) cross, (c) seagull, and (d) NP-VP diagrams. The wavy line denotes photon.

The energy shift due to the diagrams of Figs. 1(a)–1(c) is expressed as

$$\Delta E_{NP} = i(4\pi\alpha)^2 \int d^4x_1 \ldots d^4x_4 \bar{\psi}_n(x_1)\gamma^\mu S_F(x_1,x_2) \times \gamma^\nu \psi_n(x_2) D_{\mu\xi}(x_1,x_3)\Pi_N^{\xi\zeta}(x_3,x_4)D_{\zeta\nu}(x_4,x_2), \tag{1}$$

while the energy shift due to the diagram of Fig. 1(d) is expressed as

$$\Delta E_{NPVP} = -i(4\pi\alpha)^2 \int d^4x_1 d^4x_2 d^4x_3 \bar{\psi}_n(x_1)\gamma^\mu \psi_n(x_1) \times D_{\mu\xi}(x_1,x_3)\Pi_N^{\xi\zeta}(x_3,x_2)V_U(x_2)\delta_{0\zeta}\delta(t_2), \tag{2}$$

where ψ_n is the muon wave function of nth state and S_F is the muon Green's function, both constructed with the static Coulomb field from the nuclear charge together with the QED corrections due to the Uehling and Källen-Sabry effects. V_U denotes the Uehling potential. The nuclear-polarization tensor $\Pi_N^{\xi\zeta}$ of Eq. (1) contains the contact term due to the seagull diagram, while the contact term does not contribute to the energy shift due to the NP-VP diagram since the time (longitudinal) component of the NP tensor only contributes in Eq. (2). The Feynman and Coulomb gauges are employed in the photon propagator $D_{\mu\xi}$ to investigate the gauge dependence on nuclear models employed. In Eqs. (1) and (2), the photon propagator could be the dressed one by the electron-positron loops rather than the free one, in order to include the higher-order corrections associated with the NP one. So far, such a contribution has not been considered in the study of the nuclear polarization, and we have also neglected its correction in the present analysis. However, it should be noted that in the future it will be necessary to at least estimate the next leading-order contribution to confirm the convergence of the NP correction of the spin-orbit splittings.

The polarization part of $\Pi_N^{\xi\zeta}$ is constructed using the collective model. As for the transition densities of charge, the same forms are assumed for both high-lying resonances and low-lying states identified by experiment. For monopole vibrations, we employ the familiar form [16]

$$\rho_{tr}^0(r) = \sqrt{B(E0)}\frac{(3+d/dr)\rho_0(r)}{\int_0^\infty r^2 dr(3+d/dr)\rho_0(r)}, \tag{3}$$

where $\rho_0(r)$ denotes the charge density of nuclear ground states. For other modes with the multipolarity $\lambda \neq 0$, we employ the following three transition densities of Tassie-Goldhaber-Teller (TGT) [17,18], Rinker (RIN) [3], and Jensen-Steinwedel (JS) [18,19] models,

$$\rho_{tr}^{\lambda}(r) = \sqrt{B(E\lambda)}\frac{r^{\lambda-1}(d/dr)\rho_0(r)}{\int_0^\infty drr^{2\lambda+1}(d/dr)\rho_0(r)}, \quad (4)$$

$$\rho_{tr}^{\lambda}(r) = \sqrt{B(E\lambda)}\frac{r^{\lambda+1}\rho_0(r)}{\int_0^\infty drr^{2\lambda+3}\rho_0(r)}, \quad (5)$$

$$\rho_{tr}^{\lambda}(r) = \sqrt{B(E\lambda)}\frac{j_\lambda(kr/R_0)\rho_0(r)}{\int_0^\infty drr^{\lambda+2}j_\lambda(kr/R_0)\rho_0(r)}, \quad (6)$$

respectively. For the JS model, Eq. (6), $j_\lambda(kr/R_0)$ is a spherical Bessel function and k is a solution of $(d/dr)j_\lambda(kr)|_{r=R_0} = 0$ with $R_0 = 1.2A^{1/3}$. The transition densities of current for the corresponding charge densities can be obtained with the help of the continuity equation

$$i\omega_N\rho_{tr}^{\lambda(r)} = -\sqrt{\frac{\lambda}{2\lambda+1}}\left(\frac{d}{dr}-\frac{\lambda-1}{r}\right)j_{tr}^{\lambda\lambda-1}(r) + \sqrt{\frac{\lambda+1}{2\lambda+1}}\left(\frac{d}{dr}+\frac{\lambda+1}{r}\right)j_{tr}^{\lambda\lambda+1}(r), \quad (7)$$

where ω_N is the nuclear excitation energy. Using this relation, one can derive the current densities of the collective models for $\lambda \neq 0$ assuming $j_{tr}^{\lambda\lambda+1}(r) = 0$ and for $\lambda = 0$ assuming $j_{tr}^{\lambda\lambda-1}(r) = 0$.

The excitation energies and the strengths of the transition for the nuclear low-lying states are taken from the experimental data [20,21]. For the high-lying states, we assume that the response concentrates on the isoscalar and isovector giant resonances. The $B(E\lambda)$ values for these collective states are then calculated from the EWSR values and the observed peak energies [22–29]. Although the EWSR values are first estimated by the classical sum rule of Ref. [18], in the present model we allow to increase them with an enhancement factor compatible with the observed data [30]. This enhancement factor, which makes the NP corrections from the giant resonances increase, will be determined by χ^2 fits, as discussed in Sec. IV.

The PDR, which is produced by the oscillation of the neutron skin out of the phase with the core composed of equal numbers of protons and neutrons, has been identified in ^{208}Pb around 9 MeV with the strength of less than 10% of the $E1$ sum rule [8–10]. The fragment of the $E1$ strength can also be seen theoretically in ^{90}Zr around 11–12 MeV [31]. The PDR with energies 11.0 MeV in ^{90}Zr and 8.7 MeV in ^{208}Pb, are included as entries in the nuclear dipole responses in the estimation of the NP correction. We assumed that the strength ratio $B(E1;\text{PDR})/B(E1;\text{GDR}) = 0.1$. Then, we found that the PDR gives large energy shifts in ^{208}Pb; −170(TGT), −213(RIN), and −247(JS) eV for the $3p_{1/2}$ states, and −288(TGT), −359(RIN), and −416(JS) eV for $3p_{3/2}$ states, respectively, while the other muonic states are not affected as much. The reason is explained by the resonance between the muonic transition from the $3p$ to $1s$ state and the PDR mode; the muon transition energy from the $3p$ to $1s$ state in ^{208}Pb, about 8.5 MeV, canceling the excitation energy due to the PDR, provides the small energy denominator of the second-order perturbed calculation. This gives large NP energy shifts for the $3p$ states, and the $\Delta 3p$ splitting energy in muonic ^{208}Pb is reproduced, as will be shown in Sec. IV.

A similar resonant effect occurs in another muonic level of ^{208}Pb. For example, the lowlying-octupole state of ^{208}Pb at 2.617 MeV with $B(E3) = 0.612e^2\text{b}^3$ lies between the $3d_{3/2}-2p_{3/2}$ transition energy and the $3d_{5/2}-2p_{1/2}$ one. Then, the NP corrections of the muonic $3d_{3/2}$ and $3d_{5/2}$ states give a contribution with an opposite sign to each other, and therefore this nuclear state seriously affects the $\Delta 3d$ splittings. In fact, it has been known that opposite energy shifts between the muonic $3d_{3/2}$ and $3d_{5/2}$ states are essential to reproduce the $\Delta 3d$ splitting energy [5]. In the same manner as in the $3d$ levels, the dipole state of ^{208}Pb at 5.940 MeV with $B(E1) = 0.00007e^2\text{b}$, observed in $(p, p\prime\gamma)$, can resonate with the muonic $2p - 1s$ transitions, and it produces the NP corrections to $2p_{1/2}$ and $2p_{3/2}$ with an opposite sign. In this case, however, the resonant effect makes the situation of the $\Delta 2p$ anomaly worse.

In contrast to muonic ^{208}Pb, the resonant nuclear state is not provided in muonic ^{90}Zr. Since the binding energy for muonic $1s_{1/2}$ state in ^{90}Zr is about 3.6 MeV, the nuclear states with the excitation energy far from it, including the PDR, cannot resonate with muonic transitions. Moreover, even for the low-lying states observed with excitation energy less than 3.6 MeV, their energies are still too large to resonate with the muonic transitions [20]. Hence, the muonic levels in ^{90}Zr should be explained without the resonant effect.

In Table I, we now show the net NP energy shifts for the muonic levels of ^{90}Zr and ^{208}Pb, obtained by using the nuclear

TABLE I. NP corrections for muonic ^{90}Zr and ^{208}Pb (eV), in which the gauge dependencies are also shown in the parentheses. The parameters $(c, a) = (4.9608, 0.5234)$ and $(6.6577, 0.5234)$ in the Fermi-charge distribution are used for ^{90}Zr and ^{208}Pb, respectively.

^{90}Zr	$1s_{1/2}$	$2s_{1/2}$	$2p_{1/2}$	$2p_{3/2}$	$3p_{1/2}$	$3p_{3/2}$	$3d_{3/2}$	$3d_{5/2}$
TGT model	−1047(1)	−144(0)	−69(0)	−66(0)	−22.4(0.1)	−21.9(0.0)	−1.7(0.0)	−1.6(0.0)
RIN model	−1124(1)	−156(0)	−71(0)	−67(0)	−22.9(0.0)	−22.5(0.0)	−1.7(0.0)	−1.6(0.0)
JS model	−1733(7)	−243(2)	−86(0)	−81(0)	−28.2(0.0)	−27.3(0.0)	−1.7(0.0)	−1.6(0.0)
^{208}Pb	$1s_{1/2}$	$2s_{1/2}$	$2p_{1/2}$	$2p_{3/2}$	$3p_{1/2}$	$3p_{3/2}$	$3d_{3/2}$	$3d_{5/2}$
TGT model	−2727(4)	−463(1)	−1357(7)	−1425(9)	−561(4)	−749(1)	−226(0)	−43(0)
RIN model	−3599(10)	−611(4)	−1590(10)	−1656(10)	−690(3)	−914(1)	−239(0)	−42(0)
JS model	−5721(28)	−930(8)	−2178(13)	−2214(7)	−929(3)	−1179(2)	−280(0)	−38(0)

TABLE II. QED corrections for muonic ^{90}Zr and ^{208}Pb (eV). The parameters in the Fermi-charge distribution are the same as those in Table I.

^{90}Zr	$1s_{1/2}$	$2s_{1/2}$	$2p_{1/2}$	$2p_{3/2}$	$3p_{1/2}$	$3p_{3/2}$	$3d_{3/2}$	$3d_{5/2}$
eU + eKS[a]	−25764	−5009	−5956	−5624	−1818	−1736	−1439	−1411
WK[b]	+50	+16	+19	+19	+7	+7	+8	+7
mU[c]	−82	−12	−2	−1	−1	0	0	0
SE[d]	+1168	+199	−4	+37	+1	+12	−3	+2
hSE[e]	+60	+10	+5	+4	+2	+2	0	0
ES[f]	0	−2	−1	−1	−8	−8	−6	−6
Recoil[g]	−149	−21	−11	−10	−3	−2	−2	−2
^{208}Pb	$1s_{1/2}$	$2s_{1/2}$	$2p_{1/2}$	$2p_{3/2}$	$3p_{1/2}$	$3p_{3/2}$	$3d_{3/2}$	$3d_{5/2}$
eU + eKS[a]	−67864	−19537	−32648	−30082	−10871	−10334	−10605	−9941
WK[b]	+492	+244	+348	+335	+160	+160	+186	+180
mU[c]	−248	−43	−45	−34	−14	−11	−1	−1
SE[d]	+3220	+696	+348	+649	+149	+224	−44	+51
hSE[e]	+153	+25	+65	+58	+21	+20	+8	+6
ES[f]	−5	−25	−13	−13	−52	−54	−37	−39
Recoil[g]	−382	−87	−111	−95	−30	−26	−15	−14

[a]The corrections due to the unperturbed electronic Uehling and Källen-Sabry potentials.
[b]The electronic Wichman-Kroll corrections.
[c]The muonic Uehling corrections.
[d]The leading self-energy corrections.
[e]The higher-order self-energy corrections.
[f]The electron screening effect.
[g]The recoil correction.

models explained above. The nuclear charge distribution is assumed with the two-parameter Fermi distribution. All diagrams depicted in Fig. 1 are considered in the calculation, where the multipolarities up to 5^- are taken in Figs. 1(a)–1(c) and 0^+ only contributes in Fig. 1(d). The averages of the Feynman and the Coulomb gauges are listed and the differences between them are also indicated in the parentheses. In general, the gauge invariance of the NP correction is achieved separately by Fig. 1(d) only and the sum of the contributions from Figs. 1(a)–1(c), provided that the nuclear model employed is consistent. However, there is no guarantee of retaining the gauge invariance in the present calculation with collective models, where the excitation energies and $B(\mathrm{EL})$ values fitted to the observed data are used for both low-lying and high-lying states. Nevertheless, one can find that each model satisfies the gauge invariance within 1% in all muonic levels. Such a small gauge dependency is not so serious in comparison with that in Ref. [6] where the nonrelativistic RPA is used for the nuclear model. In addition, it would be very difficult to reproduce precisely the experimental low-lying states with the microscopic model, which are crucial for the NP corrections of ^{208}Pb, as discussed above. For the moment, thus, the application of the collective model rather than the microscopic nuclear model might be recommendable in the analysis of precise experimental data of muonic atoms. However, further studies with the microscopic nuclear models would be useful and should be attempted.

III. CORRECTIONS DUE TO QUANTUM ELECTRODYNAMICS

In fitting the nuclear charge parameters to the experimental transition energies, one needs to evaluate the QED corrections as well as the NP correction. The QED corrections used in our analysis are based on previous studies (see Ref. [32] and references therein). We shall summarize their treatment and numerical results below for completeness in order to make our analysis clearer.

The most important QED correction for muonic atoms is the virtual production and annihilation of the electron-positron (or particle-antiparticle) pair, the so-called vacuum-polarization (VP) correction. The VP correction arising from the electron-positron field is usually estimated by decomposing into two parts; one is the Uehling part [order $\alpha(\alpha Z)$ [33], and the other is the Wichman-Kroll (WK) one [order $\alpha(\alpha Z)^n$, $n \geqslant 2$ [34]. The Uehling potential and the electronic Källen-Sabry (KS) potential [order $\alpha^2(\alpha Z)$], which gives a part of the second-order correction [35], are added to the static Coulomb potential generating from the nuclear charge. In the present analysis, the Dirac equation of a muon is solved with the potential including the electronic Uehling and KS effects, and its muonic eigenstates are used in the perturbed calculation of the NP and self-energy (SE) corrections.

The VP corrections due to the other leptonic and the hadronic fields can also contribute for the muonic level shifts [5,32]. For example, the Uehling contribution arising from the muon-antimuon field is shown in Table II. In refitting on the muonic transition energies, we also found that this correction can be encoded into the charge parameters, that is, we can obtain an almost same χ square value whether or not this correction is considered in the analysis. Due to this fact, the other corrections such as the muonic WK correction and the hadronic VP one are neglected. Also, we neglect the mixed $\mu - e$ and hadronic$-e$ VP corrections [32]. On the other hand, the NP-VP correction of Fig. 1(d) [12], which is one of the mixed VP corrections when the vacuum loop of the electron-positron field is approximated by the Uehling part as we have done, gives a large energy shift in the muonic levels. We have already included this contribution to the muonic levels as a part of the NP correction shown in Table I.

The SE correction becomes a non-local potential and it has to be calculated as a perturbation. To estimate it with less computational effort, the nonrelativistic reduction is quite useful [36]. This method introduces a fictitious photon mass m_A chosen to satisfy the relation $(\alpha Z)^2 m_\mu \ll m_A \ll (\alpha Z)^2 m_\mu$ where m_μ is a muon mass. Then, the energy shift due to the SE correction is estimated by dividing into two terms, a high-energy term in which one may consider only a lowest order of the external field, and a low-energy one for which one may use the nonrelativistic multipole expansion, the main contribution of which is given by the dipole. We employ this method to calculate the SE correction. Although the formula is obtained by the nonrelativistic prescription, we use the relativistic matrix element to evaluate the formula in our analysis (this was already done in previous analysis using MUON2 [39]). It is well known that the mean-value method [37] employed here for the Bethe logarithm has some uncertainty [32]. Thus, the SE correction might lead to some uncertainty in the present analysis. The uncertainty of our estimate for the SE correction will be further discussed in the next section. The higher-order SE corrections are considered up to $\alpha^2 Z\alpha$ order, corresponding to the diagrams depicted in Fig. 22 of Ref. [32].

One should consider not only the vacuum correction but also the one arising from the electrons which occupy the Fermi sea. The dominant effect in such the corrections is the static electron screening between the muon and the nucleus. In the present work, we take into account only the first-order correction, in which the electron screening potential is calculated with the electron density constructed by means of the relativistic Hartree-Fock-Slater method assuming the "Z-1 approximation" [38,39].

The center-of-mass correction due to a finite nuclear mass cannot be removed rigorously in the relativistic picture. In the present analysis, the recoil effect is partially taken into account by the reduced mass of a muon and the rest is estimated approximately by the term of the Breit equation of Ref. [40].

All corrections calculated in the present analysis are summarized in Table II, where the energy shifts due to these corrections to the muonic levels in ^{90}Zr and in ^{208}Pb are shown. The energy shifts in the χ^2 analysis will vary depending on the nuclear charge parameters.

IV. RESULTS OF χ^2 ANALYSIS AND DISCUSSION

In this section, we show the results of the χ^2 analysis for the lowlying muonic transition energies with two parameters (c, a) of a Fermi charge distribution, where c denotes the half-density radius and a denotes the diffuseness parameter. Theoretical estimate of the transition energy has been done with the NP and the QED corrections described in Secs. II and III. Varying the charge parameters, these corrections, in principle, may be changed. The difficulty in performing this procedure arises from the fact that the static nuclear charge distribution is not known before the NP corrections are evaluated. Therefore, a simultaneous fit of the NP values and the charge distribution is required. Fortunately, we have been able to verify that the NP corrections are almost unchanged within the searched region of the parameters of the Fermi-type charge distribution, except for the correction due to the NP-VP diagram which is a first-order correction to the muon line. We assume here that the NP corrections due to Figs. 1(a)–1(c) are constant during the fit with respect to parameters (c, a). On the other hand, the NP-VP correction of Fig. 1(d) and all QED corrections are evaluated with the renewal of the nuclear-charge distribution.

We also consider the effect of the enhanced EWSR in the present analysis. The excessive sum rule strength is experimentally likely, though it is a difficult task to extract its value quantitatively [30]. Theoretically, the excessive strength in the observed data may be, for example, provided by the relativistic nuclear model, where the EWSR in the mean-field approximation or in the RPA is enhanced over the nonrelativistic one owing to the nucleon Dirac mass $m^* = m_N - g_\sigma \sigma$ (m_N free nucleon mass and σ scalar meson field) [41,42]. A momentum-dependent interaction and the exchange current effects in nonrelativistic models would also explain the enhancement of the EWSR.

From these viewpoints, we assume that the NP correction from the giant resonances is enhanced by a factor of x_{en} relative to the estimate of the classical EWSR values, while the NP corrections from the lowlying states are normalized by the observed transition rates. Thus the NP correction with the collective model is written as

$$\Delta E_{NP} = \Delta E_{GNP} x_{en} + \Delta E_{LNP}, \tag{8}$$

$$\Delta E_{NPVP} = \Delta E_{GNPVP} x_{en} + \Delta E_{LNPVP}, \tag{9}$$

where ΔE_{GNP} and ΔE_{GNPVP} (ΔE_{LNP} and ΔE_{LNPVP}) are the energy shifts arising from giant resonances (low-lying states). The total energy shift due to the NP correction is given by the sum $\Delta E_{NP} + \Delta E_{NPVP}$. The energy shifts of each muonic level shown in Table I are the results calculated with $x_{en} = 1.0$ and the charge parameters indicated in the caption. The χ^2 fit with respect to the charge parameters is performed for each value of the enhancement factor. Figures 2(a) and 2(b) are the results of such a χ^2 analysis (per degrees of freedom). There are nine transition energies utilized in the present analysis: $2s_{1/2} \to 2p_{3/2}, 2s_{1/2} \to 2p_{1/2}, 3p_{1/2} \to 2s_{1/2}, 3p_{3/2} \to 2s_{1/2}, 3d_{3/2} \to 2p_{3/2}, 3d_{5/2} \to 2p_{3/2}, 3d_{3/2} \to 2p_{1/2}, 2p_{1/2} \to 1s_{1/2}$, and $2p_{3/2} \to 1s_{1/2}$, given in Ref. [4] for muonic ^{90}Zr and in Ref. [5] for muonic ^{208}Pb. The previous fits using the Coulomb NP correction (CNP at $x_{en} = 1.0$) without the transverse response and PDR are very poor; $\chi^2 = 9.6$ for ^{90}Zr [4] and 188 for ^{208}Pb [5]. Considering the transverse response of nuclei, the pygmy dipole resonances, and the enhanced EWSR, discussed in Sec. II and in the present section, on the other hand, χ^2 minimums have been drastically

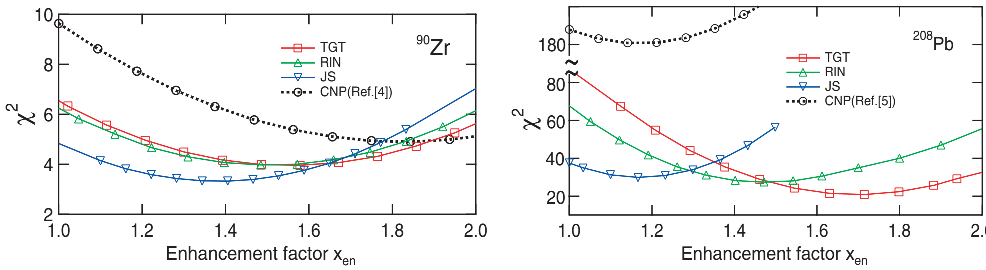

FIG. 2. (Color online) χ^2 values as a function of the enhancement factor for the EWSR (see text).

reduced to the values 3.9(TGT), 3.9(RIN), and 3.3(JS) for ^{90}Zr and 21(TGT), 27(RIN), and 30(JS) for ^{208}Pb, as seen in Fig. 2. The interesting feature in these results is the fact that the main origin of the improvement of the χ^2 fit for muonic ^{90}Zr is different from that for muonic ^{208}Pb: In ^{208}Pb, both of the transverse and the PDR effects to the nuclear polarization are quite important, while χ^2 value decreases, at most, to 180 without them, as shown by the CNP result in Fig. 2. In ^{90}Zr, on the other hand, the enhanced EWSR can decrease χ^2 of the CNP to 4.9, and the inclusion of the PDR does not change χ^2 while the transverse effect reduces χ^2 slightly.

Further, one can see in Fig. 2 that while the model-dependence of the χ^2 minimum is small, the enhancement factor giving the χ^2 minimum (optimized enhancement factor) seems to depend on the nuclear model. Actually, however, the experimental fact is simply to demand the large NP energy shifts, because, as shown in Table I and Fig. 2, the model providing the larger NP correction needs the smaller optimized enhancement factor. If the excessive strength is parametrized in terms of the effective nucleon mass, its magnitude is estimated as around $0.6m_N \sim 0.7m_N$ for TGT and RIN models and $0.75m_N \sim 0.9m_N$ for the JS model. In comparison with the analysis of the β-decay lifetimes [43] and the quadrupole resonances [44], which leads to the effective mass around $0.8m_N \sim 0.9m_N$, the result for JS model is reasonable, while the results for TGT and RIN models are inconsistent. On the other hand, the gauge dependence is least for the TGT model, while, according to the previous study comparing the collective model with the nonrelativistic RPA calculation, the RIN model gives the transition density of the charge which is nearly indistinguishable from the RPA density [3], as far as ^{208}Pb is concerned. Such behaviors of the employed models may indicate that the χ^2 minimum in the present analysis is still insufficient and that further refinement of the model would provide better results.

In order to reduce χ^2 more, it is necessary to reproduce the $2p$ splitting energy. In Table III, we compare the $\Delta 2p$ and $\Delta 3p$ splittings in the χ^2 minimum with the experimental ones. Indeed, the calculated $\Delta 2p$ splittings fall outside of the experimental error bars while the $\Delta 3p$ splittings agree within the experimental errors in both nuclei. We stress here that the PDR in ^{208}Pb has a crucial role to reproduce $\Delta 3p$ splittings. If we neglected the contribution from the PDR, the $\Delta 3p$ splitting in muonic ^{208}Pb could never be reproduced and the discrepancies of more than 50 eV would still remain for all models employed in the present calculation. Since one of the two anomalies, the anomaly in the $\Delta 3p$ splitting ^{208}Pb, has been resolved, the muonic ^{208}Pb is now in the same situation as the muonic ^{90}Zr, qualitatively.

For an explanation of the remaining discrepancy of $\Delta 2p$ splitting, an accidental resonance with an unobserved nuclear excitation state cannot be excluded *a priori* in ^{208}Pb. However, although the tendency in $\Delta 2p$ discrepancy is similar, the existence of such a resonant state is definitely excluded in ^{90}Zr. Therefore, the chance that such a resonant effect only could be responsible for the $\Delta 2p$ anomaly is small. In reducing the $\Delta 2p$ anomaly, the transverse NP effect due to the electric dipole transition with the $1s_{1/2}$ muonic intermediate state plays an important role. For $2p$ levels in ^{208}Pb, it provides a larger NP energy shift for $2p_{3/2}$ than that for for $2p_{1/2}$ state, which is necessary in order to explain the anomaly. For ^{90}Zr, however, it is not so large and the NP contribution for $2p_{3/2}$ state is still smaller than that for $2p_{1/2}$ state. As for the other NP effects which may affect the $\Delta 2p$ splitting, it remains to investigate the transverse effect of high-lying nuclear states, such as quasifree excitation and the Δ-hole resonances. While we have no reason to believe that the higher multipole contribution in the quasifree region may contribute favorably to $2p$ splittings, the effect of the Δ-hole state remains as an open question. Also, it might be important to take into account the higher-order corrections of the nuclear polarization. Such a correction is the electronic vacuum-loop correction in the virtual photon lines in Figs. 1(a)–1(c) as mentioned in Sec. II. It should be noted that, for the Δp splitting, not the absolute value but the different one of the correction between the respective states has to be discussed. Hence, the higher-order NP correction also remains as an open question.

As is shown in Table III, the remaining discrepancies for $\Delta 2p$ splittings are, considering the experimental error bar, about 5 eV for Zr and 50 eV for Pb, respectively. We should also consider the possibility that the discrepancies are caused by effects other than the nuclear polarization. In this context, one may suspect that the charge distribution of the nucleus yields model-dependence in fitting the data. The dependence on the model of charge distribution, however, seems to be negligible in the data analysis of muonic transition energies; one can verify that the χ^2 value is not reduced by using the three-parameter Fermi distribution instead of the two-parameter one. Regarding the QED corrections, the SE correction should be reexamined as is mentioned in Sec. III. From Table II, one can see that the SE correction (^{d}SE in Table II) is crucial for the Δp splitting energies.

TABLE III. Theoretical and experimental Δp splitting energies (keV) in muonic ^{90}Zr [4] and ^{208}Pb [5].

^{90}Zr level	TGT	RIN	JS	Exp.
$\Delta 2p$	21.130	21.130	21.127	21.118(8)
$\Delta 3p$	6.041	6.041	6.040	6.052(28)
^{208}Pb level	TGT	RIN	JS	Exp.
$\Delta 2p$	184.858	184.846	184.829	184.788(27)
$\Delta 3p$	47.231	47.208	47.225	47.197(45)

In particular, in ^{90}Zr, there is no other contribution that affects the splitting energy between $2p_{1/2}$ and $2p_{3/2}$ states. We have used the mean-value method [37] to estimate the Bethe logarithm in the present calculation. To see the ambiguity of this method, we have compared it with the result of the Bethe logarithm calculated by duly taking the summation over the intermediate state. The difference was at most a few percent and did not contribute to the $\Delta 2p$ fine structure splittings. Also, we have compared the relativistic matrix element used in the mean value method in the present analysis with the nonrelativistic matrix element which should be, in principle, used in the expression obtained from nonrelativistic reduction. The difference in the total magnitude of the ^{d}SE is similarly small for each level. However, the spin dependent anomalous-moment part in the SE correction is sensitive to the nonrelativistic approximation. As a result, the theoretical fine structure splittings with nonrelativistic matrix elements become larger than those given in Table III; about 20 eV for $2p$, 7eV for $3p$ in ^{208}Pb, and 2 eV for $2p$, less than the last digit for $3p$ in ^{90}Zr. In order to resolve these ambiguities, it is desirable to perform the rigorous relativistic SE calculation developed in the study of highly-charged ions [45,46]. On the other hand, since the correction due to the anomalous magnetic moment is crucial to the fine structure level splittings, we have also performed the nonperturbed calculation of the level shifts by solving the Dirac equation, as has been done for anti-protonic atoms [48]. For the muon's anomalous moment, we have used the experimental value (0.0011659214(8)(3) [47]) rather than $\alpha/4\pi$ corresponding to the lowest-order diagram considered in the present SE correction. Having performed its calculation, however, we have also verified that the present result is still unchanged. As for the QED correction of order $\alpha^2(Z\alpha)^n$, the $\alpha^2(Z\alpha)$ self-energy combined vacuum-polarization correction (^{h}SE in Table II) has been taken into account, while the virtual Delbrück effect of order of $\alpha^2(Z\alpha)^2$ has been neglected in the present analysis. The virtual Delbrück effect has a correction of order of 10 eV in muonic heavy atoms [32]. It might also be required to perform the $\alpha^2(Z\alpha)^n$ SE calculation rigorously [45,49]. As for the recoil correction, it is well known that the Breit correction we employed is correct up to $O((\alpha Z)^4)$. The formalism to carry out $O(m/M)$ correction including all orders of αZ with finite charge distribution has been recently proposed in [50], and numerical results are given for $1s_{1/2}$, $2s_{1/2}$, and $2p_{1/2}$ hydrogenlike atoms [51]. The higher order recoil correction may also affect the $\Delta 2p$ splitting, particularly in ^{208}Pb. Such a reexamination of the QED corrections would bring clarification of the problems in muonic heavy atoms.

V. SUMMARY

There has been a longstanding discrepancy between theory and experiments with regard to the fine-structure splitting energies in muonic heavy atoms. The discrepancy has been characterized by two phenomena; one is that the theoretical NP correction gave the opposite contribution to the experimentally predicted NP energy shift, and the other is that the $3p$ splitting energy of ^{208}Pb due to NP correction had to be of the same order of magnitude as the $2p$ splitting energy. In the present work our strategy to cure the former problem has been to enhance the effect of a transverse NP correction which provides a spin-dependent interaction. This is possible if the transition strengths to the high-lying states are enhanced more than the previous calculations, which is reasonable, since the observed EWSR values are larger than the classical values used in the previous analysis. For the latter problem, we have taken into account the newly established PDR, which can resonate with the muonic states through the virtual transition to $1s_{1/2}$ state. As expected, the PDR has contributed significantly to the energy shift for muonic $3p$ states in ^{208}Pb, while it has not affected the other muonic states in ^{208}Pb and all muonic states in ^{90}Zr.

Including these effects, the muonic transitions have been reanalyzed. The χ^2 minima have drastically reduced to 3.3–3.9 for ^{90}Zr and to 21–30 for ^{208}Pb. The results with the χ^2 minima in the present analysis, however, cannot be said to have reproduced all of the experimental data reasonably well. In both nuclei, particularly in ^{208}Pb, the $2p$ level splittings are not reproduced. Furthermore, the fact that the $2p$ splitting in muonic ^{90}Zr apparently could not be explained by the transverse NP effect and the excessive EWSR effect is serious since the low-lying nuclear spectra are well known and the resonant effect, which could cure the Δp anomalies, is no longer possible for ^{90}Zr. The remaining possible improvement within the NP calculation would be to evaluate the QED correction to the NP one and the correction coming from the quasifree region. A possible explanation may be found in the QED corrections performed traditionally. In particular, the SE correction has to be estimated without approximation. It is desirable to carry out all of the QED corrections consistently with a finite nuclear-matter density distribution with the same efforts as in the hydrogenlike ions, which is in principle less ambiguous than NP calculation.

ACKNOWLEDGMENTS

A. H. would like to thank Prof. Y. Tanaka for his advice on the subject of the nuclear-polarization correction and for discussing the theoretical aspects of QED corrections.

[1] V. Fitch and J. Rainwater, Phys. Rev. **92**, 789 (1953).
[2] Y. Yamazaki, H. D. Wohlfahrt, E. B. Shera, M. V. Hoehn, and R. M. Steffen, Phys. Rev. Lett. **42**, 1470 (1979).
[3] G. A. Rinker and J. Speth, Nucl. Phys. **A306**, 360 (1978).
[4] T. Q. Phan, P. Bergem, A. Rüetschi, L. A. Schaller, and L. Schellenberg, Phys. Rev. C **32**, 609 (1985).
[5] P. Bergem, G. Piller, A. Rüeetschi, L. A. Schaller, L. Schellenberg, and H. Schneuwly, Phys. Rev. C **37**, 2821 (1988).
[6] A. Haga, Y. Horikawa, and Y. Tanaka, Phys. Rev. A **66**, 034501 (2002).
[7] Y. Tanaka and Y. Horikawa, Nucl. Phys. **A580**, 291 (1994).
[8] R. D. Starr, P. Axel, and L. S. Cardman, Phys. Rev. C **25**, 780 (1982).
[9] Z. W. Bell, L. S. Cardman, and P. Axel, Phys. Rev. C **25**, 791 (1982).
[10] G. Kühner, D. Meuer, S. Müller, A. Richter, E. Spamer, O. Titze, and W. Knüpfer, Phys. Lett. **B104**, 189 (1981).
[11] Y. Horikawa and A. Haga, Phys. Rev. C **67**, 048501 (2003).
[12] L. N. Labzowsky, A. V. Nefiodov, G. Plunien, T. Beier, and G. Soff, J. Phys. B **29**, 3841 (1996).
[13] A. Haga, Y. Horikawa, and Y. Tanaka, Phys. Rev. A **65**, 052509 (2002).
[14] J. L. Friar and M. Rosen, Ann. Phys. (NY) **87**, 289 (1974).
[15] R. Rosenfelder, Nucl. Phys. **A393**, 301 (1983).
[16] P. Ring and P. Schuck, *The Nuclear Many-Body Problem* (Springer-Verlag, Berlin, 1980), p. 336.
[17] L. J. Tassie, Austral. J. Phys. **9**, 407 (1956).
[18] A. Bohr and B. R. Mottelson, *Nuclear Structure* (Benjamin, New York, 1975), Vol. 2, p. 325.
[19] G. Plunien, B. Müller, W. Greiner, and G. Soff, Phys. Rev. A **39**, 5428 (1989); **43**, 5853 (1991).
[20] E. Browne, Nucl. Data Sheets **82**, 379 (1997).
[21] M. J. Martin, Nucl. Data Sheets **47**, 797 (1986).
[22] D. H. Youngblood, H. L. Clark, and Y.-W. Lui, Phys. Rev. Lett. **82**, 691 (1999).
[23] D. H. Youngblood, Y.-W. Lui, B. John, Y. Tokimoto, H. L. Clark, and X. Chen, Phys. Rev. C **69**, 054312 (2004).
[24] A. Erell, J. Alster, J. Lichtenstadt, M. A. Moinester, J. D. Bowman, M. D. Cooper, F. Irom, H. S. Matis, E. Piasetzky, U. Sennhauser, and Q. Ingram, Phys. Rev. Lett. **52**, 2134 (1984); A. Erell, J. Alster, J. Lichtenstadt, M. A. Moinester, J. D. Bowman, M. D. Cooper, F. Irom, H. S. Matis, E. Piasetzky, and U. Sennhauser, Phys. Rev. C **34**, 1822 (1986).
[25] J. D. Bowman, *Nuclear Structure* (North-Holland, Amsterdam, 1985), p. 549.
[26] B. L. Berman and S. C. Fultz, Rev. Mod. Phys. **47**, 713 (1975).
[27] D. H. Youngblood, Y. -W. Lui, H. L. Clark, B. John, Y. Tokimoto, and X. Chen, Phys. Rev. C **69**, 034315 (2004).
[28] D. S. Dale, R. M. Laszewski, and R. Alarcon, Phys. Rev. Lett. **68**, 3507 (1992).
[29] M. A. Godwin, E. Hayward, G. Feldman, L. H. Kramer, H. R. Weller, and W. R. Dodge, Phys. Rev. C **50**, 1528 (1994).
[30] D. H. Youngblood, Phys. Rev. C **55**, 950 (1997).
[31] Z. -Y. Ma, H. Toki, and N. Van Giai, Nucl. Phys. **A627**, 1 (1997).
[32] E. Borie and G. A. Rinker, Rev. Mod. Phys. **54**, 67 (1982).
[33] E. A. Uehling, Phys. Rev. **48**, 55 (1935).
[34] E. H. Wichmann and N. M. Kroll, Phys. Rev. **101**, 843 (1956).
[35] G. Källen, A. Sabry, and K. Dan. Vidensk. Selsk. Mat.-Fys. Medd. **29**, No. 17 (1955).
[36] R. C. Barrett, Phys. Lett. **B28**, 93 (1968).
[37] G. A. Rinker and L. Steffen, At. Data Nucl. Data Tables **20**, 143 (1977).
[38] J. B. Mann and G. A. Rinker, Phys. Rev. A **11**, 385 (1975).
[39] G. A. Rinker, Comput. Phys. Commun. **16**, 221 (1979); Y. Tanaka, the formalism of MUON2 and XRAY2, Los Alamos National Laboratory (1984) (unpublished).
[40] J. L. Friar and J. W. Negele, Phys. Lett. **B46**, 5 (1973).
[41] C. E. Price and G. E. Walker, Phys. Lett. **B155**, 17 (1985).
[42] J. A. McNeil, R. J. Furnstahl, E. Rost, and J. R. Shepard, Phys. Rev. C **40**, 399 (1989); J. R. Shepard, E. Rost, and J. A. McNeil, *ibid.* **40**, 2320 (1989).
[43] T. Nikšić, T. Marketin, D. Vretenar, N. Paar, and P. Ring, Phys. Rev. C **71**, 014308 (2005).
[44] P.-G. Reinhard, Nucl. Phys. **B649**, 305c (1999).
[45] P. J. Mohr, G. Plunien, and G. Soff, Phys. Rep. **293**, 227 (1998).
[46] A. M. Desiderio and W. R. Johnson, Phys. Rev. A **3**, 1267 (1971); P. J. Mohr, Ann. Phys. (NY) **88**, 26 (1974); K. T. Cheng and W. R. Johnson, Phys. Rev. A **14**, 1943 (1976); K. T. Cheng, W.-D. Sepp, W. R. Johnson, and B. Fricke, *ibid.* **17**, 489 (1978); I. Lindgren, H. Persson, S. Salomonson, and A. Ynnerman, *ibid.* **47**, R4555 (1993); H. M. Quiney and I. P. Grant, J. Phys. B **27**, L299 (1994).
[47] G. W. Bennett, *et al.*, Phys. Rev. Lett. **92**, 161802 (2004).
[48] E. Borie, Phys. Rev. A **28**, 555 (1983).
[49] H. Persson, I. Lindgren, L. N. Labzowsky, G. Plunien, T. Beier, and G. Soff, Phys. Rev. A **54**, 2805 (1996).
[50] V. M. Shabaev, Teor. Mat. Fiz. **63**, 394 (1985); Phys. Rev. A **57**, 59 (1998).
[51] A. N. Artemyev, V. M. Shabaev, and V. A. Yerokhin, Phys. Rev. A **52**, 1884 (1995); V. M. Shabaev, A. N. Artemyev, T. Beier, G. Plunien, V. A. Yerokhin, and G. Soff, *ibid.* **57**, 4235 (1998).